STUDY ON REFLECTION AND TRANSMISSION COEFFICIENTS OF COMB-TYPE CAISSON BREAKWATER

XIN-YU WANG[1], YONG LIU[2]
[1]*Shandong Provincial Key Laboratory of Ocean Engineering, Ocean University of China, Qingdao 266100, China, wangxinyutykc@126.com*
[2]*Shandong Provincial Key Laboratory of Ocean Engineering, Ocean University of China, Qingdao 266100, China, liuyong@ouc.edu.cn*

Abstract: This paper presents a three-dimensional (3-D) numerical solution of nonlinear wave interactions with comb-type caisson breakwaters. The numerical solution is developed by the open-source CFD library OpenFoam® which contains a C++ toolbox called waves2Foam for solving free surface Newtonian flows using the Reynolds averaged Navier-Stokes equations with volume of fluid method (VOF) tracking the free surface. Relaxation zone technique is implemented to avoid wave reflection from marine structure and outlet boundaries by applying relaxation functions inside the relaxation zone. The second-order Stokes wave theory are adopted to generate nonlinear wave trains in the inlet relaxation zone. The numerical solution is obtained in a strip of fluid domain for the saving of computational cost by using two different boundary conditions: symmetryPlane in a planar for the front and back faces of the fluid domain and symmetry in non-planar for the wall of comb-type caissons and side plates. In order to investigate the energy dissipation from fluid viscosity, an analytical solution based on potential theory for the present problem is compared with the numerical solution. The results show that the comb-type caisson breakwater can dissipate wave energy efficiently and thus present a good sheltering for harbour basin. The present numerical model is expected to be an efficient tool for preliminary design of comb-type caisson breakwater (periodical marine structures).

Keywords: *Comb-type caisson, Numerical simulation, Reflection coefficient, Transmission coefficient, Energy dissipation*

1. Introduction

A comb-type caisson consisting of a rectangular caisson and two partially immersed side plates (see Figure 1) has been invented and successfully used for building a breakwater in Da-yao Bay of Dalian, China (Niu et al., 2003). Compared with traditional rectangular caissons, the comb-type caisson can save engineering investment and reduce the requirement of foundation bearing capacity, as the rectangular caisson is partially replaced by side plates (Niu et al., 2001). Most of all, the gap beneath the side plates allow the partially pass of tide current, and thus significantly reduce the flow velocity near the breakwater entrance and guarantee the navigation safety. In addition, the reflection coefficient and wave forces acting on the comb-type caisson breakwater are smaller than that of the traditional caisson breakwater, and thus the stability against sliding of the structure can be enhanced (Li et al., 2002).

The wave interactions with comb-type caisson breakwaters have been investigated by some scholars using experimental tests and numerical methods. The working mechanism of comb-type caisson breakwater and its sheltering function were summarized by Zhu et al. (2001). The hydrodynamic performance of comb-type caisson breakwaters has been examined by Li et al. (2002) and Dong et al. (2003), and an empirical formula for calculating the horizontal wave forces acting on comb-type caisson breakwaters has been developed. Wang et al. (2001) analysed the stress characteristics of side plates and carried out model tests on wave forces acting on side plates to analyse its structure and structure reinforcement design. The internal stress distribution, the natural vibration characteristics and static forces of side plates were examined by Zhang et al. (2002) using finite element method. Fang et al. (2011) developed a three-dimensional numerical wave tank using Fluent to examine the hydrodynamic performances of comb-type caisson breakwaters, and gave an empirical formula to estimate the transmission coefficient. Wang et al. (2017) developed a three-dimensional analytical solution to solve wave scattering by the comb-type caisson breakwater, and gave theoretical formulae for the reflection and transmission coefficients.

Although some studies on the comb-type breakwater have been performed, numerical analysis on comb-type caisson breakwaters are still not enough. This paper will develop an efficient 3-D numerical solution for nonlinear wave interactions with comb-type caisson breakwaters using symmetry and symmetryPlane boundary conditions. A better understanding on the hydrodynamic performance of the comb-type caisson breakwater after considering fluid viscosity and nonlinear wave may be presented by the present numerical study. In the following section, a numerical solution is presented in detail, which is capable of solving wave scattering by comb-type caisson breakwater and other periodical marine structures. In section 3, the numerical model is validated and typical numerical results are presented and discussed. Finally, the main conclusions of this study are drawn.

2. Numerical Model

2.1 Governing equations

The governing equations for the combined flow of air and water phases are given by the incompressible continuity equation and momentum equations:

$$\nabla \cdot \mathbf{U} = 0 , \tag{1}$$

$$\frac{\partial \rho \mathbf{U}}{\partial t} + \nabla \cdot (\rho \mathbf{U}\mathbf{U}^T) - \nabla \cdot (\mu \nabla \mathbf{U}) = -\nabla p^* + g \cdot (\mathbf{x} - \mathbf{x}_r)\nabla \rho , \tag{2}$$

where the bold fonts indicate a vector field. $\mathbf{U}$ is the velocity vector field; ρ is the fluid density; μ is the dynamic viscosity;

p^* is the dynamic pressure; $\mathbf{x}$ is the Cartesian coordinate vector, $\mathbf{x}_r$ is a reference location related to still water level.

The above governing equations for viscous fluid are simultaneously solved using waves2Foam (interFoam solver). The waves2Foam tracks the movement of the interface between air and water phases by the VOF technique (Jacobsen et al., 2015). The volume fraction α is bounded from 0 to 1 where $\alpha = 0$ means air full of cell and $\alpha = 1$ means water full of cell and any intermediate value is a mixture of air and water. The density and viscosity fields are all calculated based on the volume fraction field, which satisfies:

$$\frac{\partial \alpha}{\partial t} + \nabla \cdot \mathbf{U}\alpha + \nabla \cdot (\mathbf{U}_r \alpha(1-\alpha)) = 0 \,, \tag{3}$$

where, the last term at the left hand is the interface compression term to avoid the excessive diffusion of the interface, and $\mathbf{U}_r$ is a compressive velocity. The pressure and velocity fields are obtained by solving Eqs. (1) and (2), while the free surface is captured with Eq. (3).

2.2 Solving procedure

In OpenFoam, Finite volume method is employed to discretize the governing equations. In the discretization process, different interpolation schemes are adopted to discretize each term of governing equations. For instance, the implicit Euler scheme is always used for the first term of momentum equation. This scheme is a first order accuracy in time and provides relatively accurate results with small time steps. More information is introduced in Moukalled et al. (2015).

The numerical procedure for the waves2Foam is summarized as follows. First, we solve the transportation Eq. (3) equation for volume fraction field. In the process of solving the volume fraction, a numerical method called Mules (Multidimensional Universal Limiter for Explicit Solution) is applied in waves2Foam. This method is more efficiency because it introduces an artificial convection term $\nabla \cdot (\mathbf{U}_r \alpha(1-\alpha))$ developed by Weller (2002) to ensure a sharp interface rather than reconstructing the free surface in each time step. And then the values of fluid and interface properties are updated based on volume fraction field. At last, the discretized governing equations are solved using PIMPLE algorithms.

The numerical algorithm PIMPLE is adopted in numerical model combining two algorithms PISO (Pressure-Implicit Splitting of Operators) and SIMPLE (semi-implicit method for pressure-linked equations). For the implementation of PIMPLE algorithm, the transient term of solution between two time steps is solved by PISO algorithm while the steady-state flow is obtained using SIMPLE algorithm in each time step. The advantage of PIMPLE algorithm is to speed up numerical simulation by using under relaxation factor with a relative big time step. PISO and SIMPLE algorithms are thoroughly explained in Jasak (1996).

2.3 Numerical wave flume

The comb-type caisson breakwater comprised of an array of uniform comb-type caissons is plotted (only six entire caissons) in Fig. 1. It can be seen from Fig.1 that the width of a wave chamber formed by adjacent rectangular caissons and partially immersed side plates is *B*. The water depth is of constant *d* and the bottom of side plate is at a distance of *b* away from the seabed with a side plate height h_a ($h_a = d - b$). The composition for one unit of comb-type caisson is shown in upper left corner of Fig. 1. The length of rectangular caisson is *c*, and the length of side plate is *a*. Figure 2 shows the 3-D numerical wave flume with a model of comb-type caisson and the Cartesian coordinate system is chosen. The wave flume was set up in 25 m long, 1.5 m high and 1.6 m wide and divided into three zones: inlet relaxation zone I, zone II with one unit of comb-type caisson and inlet relaxation zone III. Waves with wave height *H* and wavelength *L* are normally incident. The origin is located at the intersection of inlet face, seabed face and front face. Thus, the *x*-*y* plane is in the seabed at $z = 0$ and *y*-axis points vertically upwards along the inlet surface with the still water level at $y = 1$ m.

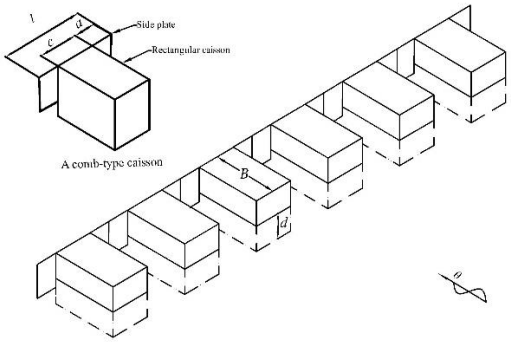

Fig. 1 Idealized sketch for wave interaction with a comb-type caisson breakwater

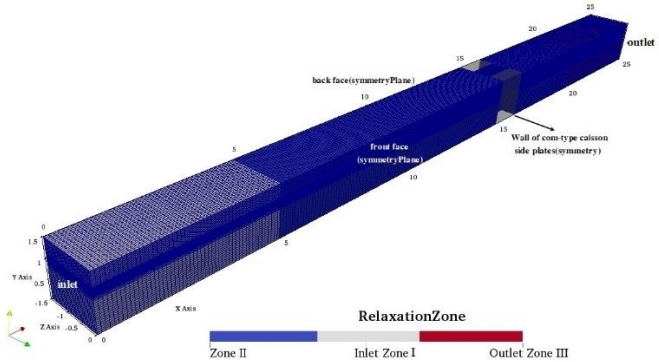

Fig. 2 The sketch of 3-D wave flume with a comb-type caisson

In Fig. 3, a 2-D sketch is plotted to present the vertical cross section created along $z = -0.8$ m of the 3-D wave flume in Fig.2. The vertical cross section is located at the middle of the side plate. Three horizontal zones with identical cell size grading have been defined. The inlet relaxation zone I represents the wave propagation and absorption area, and covers from $x = 0$ m to $x = 5$ m. The zone II is located from $x = 5$ m to $x = 20$ m. The comb-type caisson lies between 15 m and 16.25 m as show in Fig. 3. The thickness of the side plate Δx_t is set to 0.05 m. The outlet relaxation zone III covers the final 5 m where the wave energy is totally absorbed. In the *y*-direction the cell size is constant and equal to 1 cm throughout the flume.

2.4 Generation of mesh refinement

The mesh refinement is created with snappyHexMesh at a band from y = 0.9 m to 1.1 m around free surface elevation. The grid cells are refined in all directions by splitting the original cells in quarter. This mesh refinement scheme saves computational cost by having less cells. A numerical investigation without marine structure are implemented to study the effect of different mesh sizes on the numerical results at x=15 m in Fig. 4. It can be seen from Fig. 4 that slight wave attenuations occur in sparse grid where sparse grid spacing (Δx_s = 0.05 m) in x-direction is a fifth of refinement grid spacing (Δx_r). But, we can obtain a target wave height H = 0.05 m for sparse grid at breakwater area when we set an appropriate inlet wave height. Therefore, for high efficiency in computations, the mesh level Δx_s is adopted in following simulations.

The results of numerical solution can be obtained in a strip of one comb-type caisson unit instead of calculating the whole fluid domain owing to adopting two different boundary conditions: one is called symmetryPlane in a planar for the front and back face of the fluid domain and the other is called symmetry in non-planar for the wall of comb-type caissons and side plates. The numerical boundary conditions utilized in this model can improve computational efficiency considerably.

Table 1 The list of wave parameters, dimensions of comb-type caisson element and locations of wave gauges.

Dimensions of comb-type caisson		Numerical wave parameters	wave gauges points(WGP) (x, y, z) unit(m)			
A	0.3 m	wave theory: Stokes waves	0	(0, 0.9~1.1, -0.8)	4	(10, 0.9~1.1, -0.8)
C	1.0 m	wave height: 0.05 m, 0.08 m	1	(3, 0.9~1.1, -0.8)	5	(16.5, 0.9~1.1, -0.8)
B	0.5 m	water depth: 1 m	2	(8, 0.9~1.1, -0.8)	6	(22, 0.9~1.1, -0.8)
B	1.2 m	wave period: 1.2 s, 1.8 s	3	(9, 0.9~1.1, -0.8)	7	(24, 0.9~1.1, -0.8)

3. Numerical results

3.1 Validations of numerical model

The present numerical model is validated from two aspects, including the generation of linear and nonlinear wave trains and interactions between waves and comb-type caisson breakwaters. The dimensions of comb-type caisson structure, wave parameters and wave gauge points (WGP) utilized in the following calculations are listed in Table 1.

Linear wave train with H = 0.05 m and T =1.8 s and non-linear second-order stokes wave train with H = 0.08 m and T = 1.2 s are generated in the wave flume without marine structure. The corresponding numerical results of wave surface elevations are compared with the theoretical results in Fig. 5 and Fig. 6, respectively. It is noted that the time series of free surface elevations for numerical solution are in good agreement with that of theoretical solution at x = 0 m and 3 m. The wave heights are reduced effectively at x = 22 m and almost vanished at x = 24 m because the wave gauge locations are inside outlet relaxation absorption zone. Thus, the effectiveness of the relaxation zones at the inlet and outlet is confirmed. It is also noted in Fig. 6 that the mean water level of the numerical solution has a slight increase at the entire time instance because of the nonlinear resonant wave interactions (Chapalain et al., 1992).

In Fig.7, the wave forms with x = 11 m and 13 m are also plotted to verify the nonuniformity of the numerical wave flume at z = -0.4 m and -0.8 m. It can be seen that the wave forms at two z-directions are in good agreement at x = 11 m before t = 22 s. But for t > 22 s a slight difference in the wave forms appears due to the phase shift resulting from the periodical structure along z-directions. We can also observe that at x = 13 m the wave forms at z = -0.4 m and -0.8 m do not exactly coincide after t = 17 s. But the difference between x = 11 and 13 m is that the non-overlapping phenomenon appears earlier at x =13 m due to the shorter distance from the front wall of the breakwater.

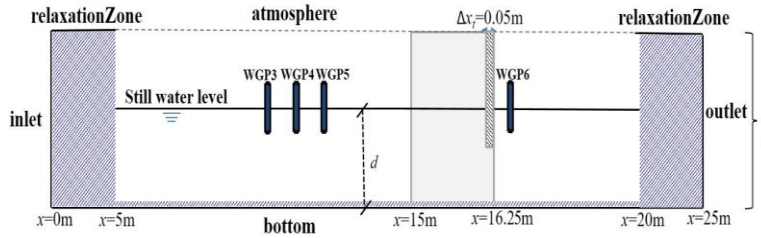

Fig. 3 A 2-D sketch of vertical cross section along z = -0.8 m of the 3-D wave flume.

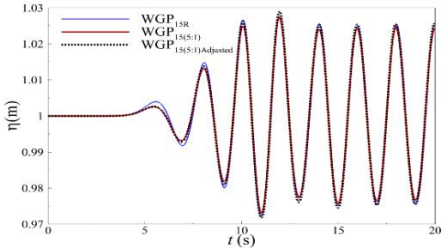

Fig. 4 Free surface elevations of linear wave at WGP (x = 15 m) for two different grid sizes.

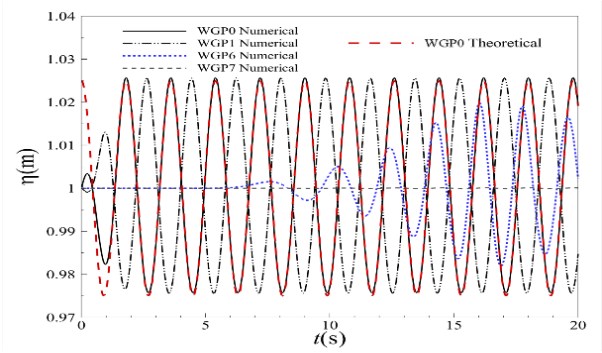

Fig. 5 Free surface elevations at the WGP of linear waves.

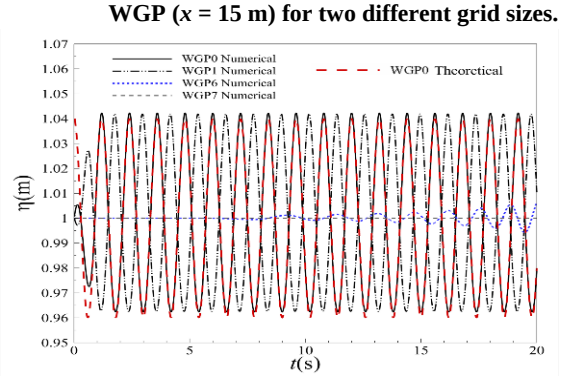

Fig. 6 Free surface elevations at the WGP of second-order Stokes waves.

3.2 Discussions

Comparisons between the present numerical results and the analytical solution (Wang et al., 2017) for the reflection coefficients C_r and the transmission coefficients C_t at different heights of side plates are plotted in Fig. 8 and Fig. 9, respectively. The reflection coefficients of numerical solution are determined by the method of Goda and Suzuki (1976). It can be seen from Figs. 8 and 9 that the curves of C_r and C_t calculated by the two different methods have the same variation trend with the increasing value of h_a. But the numerical results are smaller than that of the analytical solution as the fluid viscosity (energy dissipation) has been well considered in the numerical solution. In Fig.10, the quadratic sum of the reflection and transmission reflections ($C_r^2 + C_t^2$) for the numerical reuslts is plotted. It is noted that the value of $C_r^2 + C_t^2$ for the analtyical solution always equals to unity due to zero energy loss in analytical solution. Thus it is not plotted. For the numerical result in Fig. 10, the curve of $C_r^2 + C_t^2$ first decreases and then increases with the increasing value of h_a. In general, the side plate heights have significant effect on the hydrodynamic performance of comb-type breakwaters and should be carefully taken into account in the engineering design.

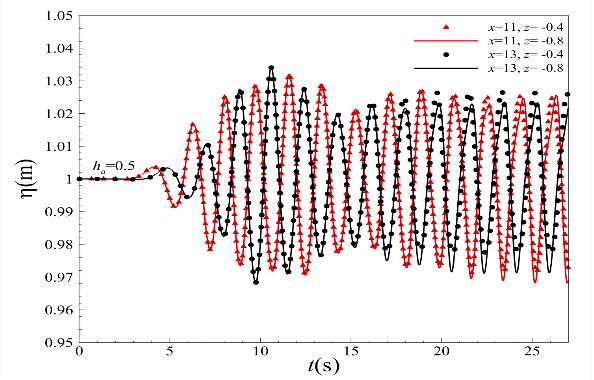

Fig. 7 Wave surface elevations at different locations.

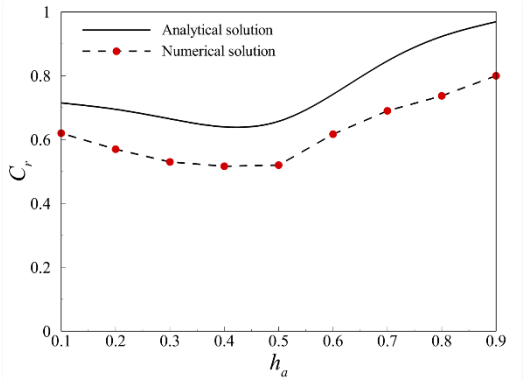

Fig. 8 Comparison between the analytical and the numerical results of C_r.

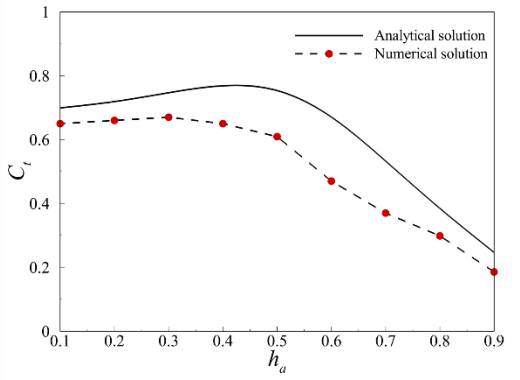

ig. 9 Comparison between the analytical and numerical results of C_t.

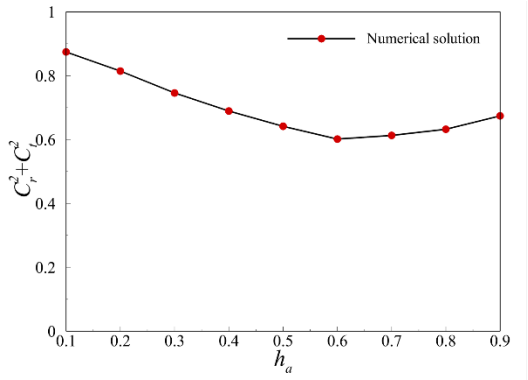

Fig. 10 Variations of the quadratic sum of C_r and C_t versus the heights of side plate.

4. Conclusion

In this study, a 3-D numerical solution for problems regarding wave generation, absorption and wave interacting with comb-type caisson breakwaters has been developed based on OpenFOAM®. The present method is very efficient to investigate water wave scattering by periodical structures because of the application of symmetry and symmetryPlane boundary conditions. The wave surface elevations generated in the numerical wave flume have been carefully examined and confirmed. The variation of the numerical results for the reflection and transmission coefficients versus the side plate height is similar to that of the analytical solution based on linear potential theory, while the value of the numerical solution is much smaller due to energy dissipation by the fluid viscosity. The reflection and transmission coefficients and the energy dissipation due to fluid viscosity are significantly affected by the height of side plate. The present numerical solution will be further validated by experimental data in the next study.

Reference

[1] Chapalain G, Cointe R, Temperville A. Observed and modeled resonantly interacting progressive water-waves. Coastal Engineering, 1992, 16(3):267-300.

[2] Dong, G. H., Li, Y. C., Sun, Z. C., Sun, Y., Niu, E. Z. and Mao, K., Interaction between waves and a comb-type breakwater. China Ocean Engineering, 2003, 17(4), 517-526.

[3] Fang, Z., Zhang, N. C., and Zang Z. P., Numerical simulations of open comb-type breakwater and research on its wave transmission coefficient. Journal of Waterway and Harbor, 2011, 32(2):86-93.

[4] Goda, Y., Suzuki, Y. Estimation of incident and reflected waves in random wave experiments. Proc. of 15th Int. Coastal Eng. Conf., 1976, 828–845.

[5] Jacobsen, N.G., Fuhrman, D. R., and Fredsøe, J. A wave generation toolbox for the open-source CFD library: OpenFoam®. International Journal for Numerical Methods in Fluids, 2012, 70(9), 1073–1088.

[6] Jasak, H. Error analysis and estimation for the finite volume method with applications to fluid flows. Ph.D. thesis, Imperial College of Science, Technology and Medicine, 1996.

[7] Li, Y. C., Sun, Z. C., Xu, S. Q., Dong, G. H., Lin, Y. Z., Niu, E. Z. and Mao, K., The hydraulic performance of comb-type vertical breakwater. Journal of Hydrodynamics, Ser. A, 2002, 17(4), 472-482. (In Chinese with English abstract)
[8] Moukalled F, Mangani L, Darwish M. The Finite Volume Method in Computational Fluid Dynamics: An Advanced Introduction with OpenFOAM and Matlab, Springer Publishing Company, Incorporated, 2015.
[9] Niu, E. Z., Ma, D. T. and Sun, S. C., The novel Comb-type breakwater. China Civil Engineering Journal, 2003, 36(10), 51-56. (In Chinese with English abstract)
[10] Niu, E. Z., Deng, L. and Ma, D. T., Experimental studies and construction of comb-type breakwater. China Harbour Engineering, 2001, 6, 5-8. (In Chinese with English abstract)
[11] Wang, Q. X., Zhang, T., Zhao, G. F. and Niu, E. Z., Structure analysis for flange plate of Comb-type caisson. China Harbour Engineering, 2001, 3, 13-17. (In Chinese with English abstract)
[12] Wang, X. Y., Liu, Y., Study on reflection and transmission characteristics of comb-type caisson breakwater. 18th Academic Symposium on the China Ocean (offshore) project, 2017. (In Chinese with English abstract)
[13] Weller, H.G., Derivation, modelling and solution of the conditionally averaged two-phase flow equations. Technical Report TR/HGW/02. Nabla Ltd., 2002.
[14] Zhu, H., Niu, E. Z. and Zheng, T. L., Mechanism and Characteristics of Comb-type Open Breakwater and Its Sheltering Effect. Port & Waterway Engineering, 2001, 10, 008. (In Chinese with English abstract)